Synchronized Conformational Fluctuations and Binding Site Desolvation during Molecular Recognition†

Sutjano Jusuf and Paul H. Axelsen*

Departments of Pharmacology, Biochemistry, and Biophysics, University of Pennsylvania, Philadelphia, Pennsylvania 19104

Received July 31, 2004; Revised Manuscript Received September 13, 2004

ABSTRACT: Binding site desolvation is a poorly understood prerequisite to ligand binding. Although structural fluctuations may be expected to have an important role, little is known about which fluctuations are important or the mechanism by which they promote desolvation. This investigation examines whether and how specific structural fluctuations contribute to desolvation of the ligand binding site in glycopeptide antibiotics. Backbone peptide group rotations in vancomycin, known to occur by experimental observation, were examined in this work with a two-dimensional adaptive umbrella sampling molecular dynamics simulation technique. Results indicate that energetic barriers to rotation are relatively small for two of the peptide groups intimately involved in ligand recognition. When they occur, these rotations strip water molecules away from key hydrogen bond donors and simultaneously cause significant distortions in the macrocyclic rings of the antibiotic that force water into and out of the binding site. Both events are intricately synchronized on the molecular level and have consequences that are clearly necessary to prepare the binding site for receiving a ligand. These results suggest that previously reported observations concerning structural dynamics and binding kinetics in these compounds are mechanistically linked, and they illustrate a heretofore unrecognized degree of preorganization, complexity, and synchronization that may be involved in specific molecular recognition. They also suggest that strategies for increasing antibiotic affinity through covalent dimerization may be counterproductive.

A key requirement for the formation of a biomolecular complex is desolvation, i.e., the removal of solvent from atoms that comprise the ligand binding interface. Even the simplest case, nonspecific association between two convex surfaces, for example, involves considerable complexity because the replacement of surface-adsorbed solvent with ligand requires overcoming hydration forces and double layer effects (*1*). A "zippering" mechanism has been proposed in which desolvation and binding occur in a concerted fashion (*2*). This mechanism is plausible for superficial binding sites, but it does not explain how ligands might replace solvent in the more typical situation of a binding site that is deeply situated with a narrow entrance channel. It seems likely that desolvation mechanisms in such circumstances involve conformational flexibility. We hypothesize that large-scale dynamics in a protein may promote desolvation by destabilizing solvent structure within the binding site and regulating the bulk flow of solvents in and out of the binding pocket.

In this work, we have examined the role of large-scale dynamics in desolvating the ligand binding site of vancomycin. Vancomycin is a glycopeptide antibiotic that binds to polypeptide segments terminating in D-alanyl-D-alanine (Figure 1). It is one of the smallest natural products that exhibit stereospecific molecular recognition. Experimental stopped-flow studies of vancomycin binding kinetics indicate that binding is a two-step process. The fast initial step is thought to involve the formation of a loose initial binding complex, while a slower rate-determining step is more likely to involve a conformational rearrangement (*3*). This conformational rearrangement is unlikely to involve rotation of the charged N-terminal residue or the disaccharide group. Therefore, it is of interest that other experimental studies employing NMR have shown that the peptide group between amino acid residues 2 and 3 is found in two different orientations (*4*). In one orientation, the amide hydrogen of residue 3 is in the binding site and positioned suitably for hydrogen bond formation with a ligand. In the other orientation, the peptide group is rotated by ∼180° and the amide hydrogen is oriented away from the binding site. The presence of two distinct conformations suggests that the peptide group can rotate, which in turn implies that either the amide hydrogen of residue 3 or the carbonyl oxygen of residue 2 must pass through the macrocyclic ring. This investigation focuses on the nature of conformational rearrangements in vancomycin as a consequence of these rotations and their role in facilitating binding site desolvation through destabilization of solvent structure.

A complete free energy potential surface for rotation of backbone peptide groups can, in principle, be obtained from an ordinary molecular dynamics (MD) simulation. However, transitions between low-energy conformations may not occur within the time scales that are currently accessible by MD simulation. Consequently, simulations tend to sample only a rather limited set of conformations accessible only from the initial atomic positions and velocities. To more thoroughly explore the conformational space available to van-

† This work was supported by Grant AI43412 from the National Institutes of Allergy and Infectious Diseases.

* To whom correspondence should be addressed. Tel: (215) 898-9238. Fax: (215) 573-9135. E-mail: axe@pharm.med.upenn.edu.

10.1021/bi048357t CCC: $27.50
Published on Web 11/18/2004

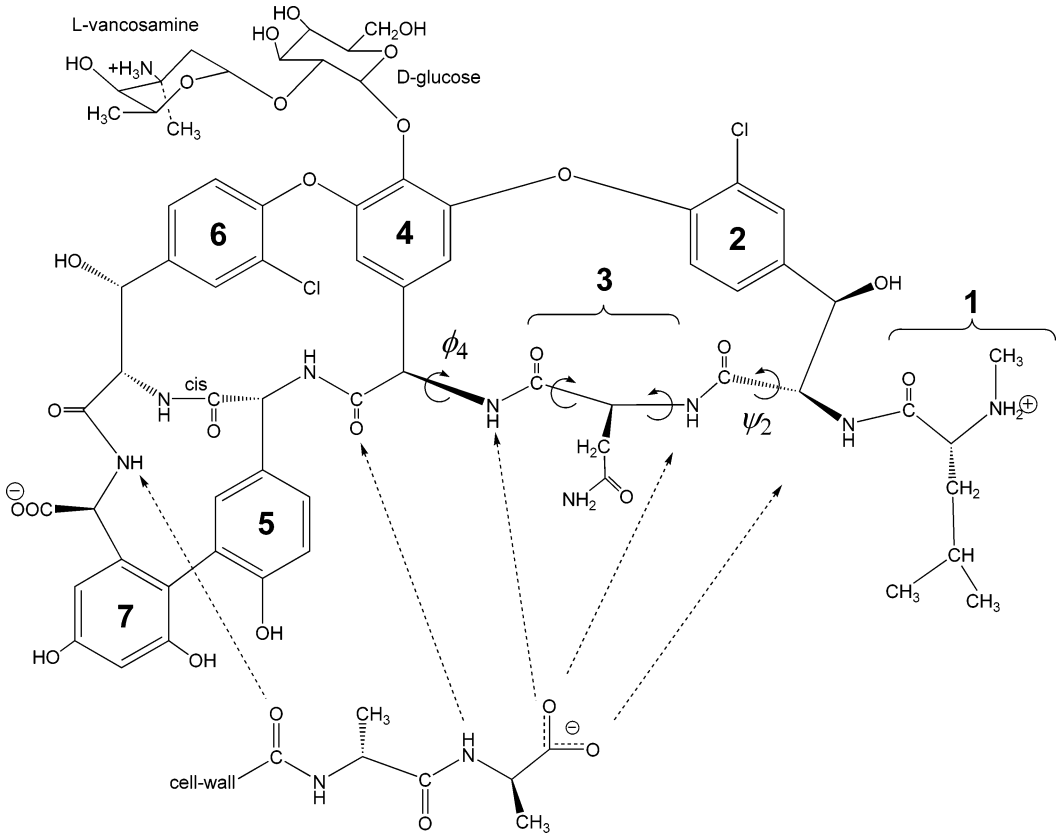

FIGURE 1: Vancomycin and the C-terminal bacterial cell wall intermediate D-Ala-D-Ala. The amino acid residues in vancomycin are numbered 1−7. Hydrogen bonds that form between vancomycin and the cell wall intermediate are depicted in dotted lines. The torsion angles monitored during an umbrella sampling are labeled ψ_2 and ϕ_4; however, it should be noted that both rotations are accompanied by a corresponding rotation on the other side of the peptide group so that the peptide group remains in a trans configuration.

comycin, we have applied an adaptive umbrella sampling simulation technique (*5*) to the rotation of two peptide groups in vancomycin. Results show that barriers to the rotation of two different backbone peptide groups are sufficiently small that they may be readily crossed at ordinary temperatures. These rotations contribute to desolvation of the ligand binding site by destabilizing water structure, stripping hydrogen-bonded water from peptide groups involved in molecular recognition, and expelling water from the binding site to make ligand entry possible.

METHODS

Simulation Protocol. Molecular dynamics simulations were performed using CHARMm (*6*) version c30b1 with atom types and all-hydrogen parameters as described previously (*7*−*11*). The TIP3P water model was used with periodic boundary dimensions of 40 × 40 × 40 Å^3. Electrostatic interactions were calculated using the particle mesh Ewald (PME algorithm), a β-spline order of 6, an FFT grid of one point per (64 × 64 × 64) Å, and a real space Gaussian width κ of 0.4 Å^{-1}. van der Waals interactions were truncated using an atom-based cutoff at 12 Å. Dynamic trajectories were generated at a constant pressure and temperature (1.0 atm and 300 K) (*12*). SHAKE was used throughout, and the equation of motion was integrated with a time step of 1 fs (*13*). Coordinates were saved every 50 fs for analysis.

System Specifications. The starting coordinates of a vancomycin monomer were derived from the 0.89 Å resolution crystal structure of a monomer with a bound acetate ligand from a previously published vancomycin dimer:acetate structure (Protein Data Bank entry 1AA5) (*14*). One chloride ion from the crystal structure was included for overall charge neutrality but positioned as far as possible from any vancomycin image. This system was placed at the center of a 40 × 40 × 40 Å cubic array of water molecules, and overlapping waters within 2.8 Å of any system component were deleted. The resulting system contained a total of 2062 water molecules. Water positions were equilibrated for 10 ps at 300 K while the vancomycin monomer was constrained to its initial coordinates. The monomer was then released, and the system was propagated for an additional 490 ps. The final positions and velocities from this 500 ps conditioning period were used to launch a 1 ns unbiased simulation and a series of adaptive umbrella sampling calculations totaling 2.4 ns.

Adaptive Umbrella Sampling. In unbiased molecular dynamics simulations, peptide group rotation is an infrequent event. Therefore, an adaptive umbrella sampling technique was employed to characterize the potential of mean force (pmf) (*5*). In this technique, a series of simulations are performed in which an umbrella potential is progressively adjusted to yield a uniform distribution along the selected degree of freedom. Accordingly, the pmf sought is the negative of the umbrella potential.

Given sets of system coordinates sampled at regular time intervals during a simulation, the number of coordinate sets along a selected degree of freedom is counted into k bins of equal sizes. Using the distribution of counts from a series of umbrella sampling runs j, the unbiased probability distribution P_k is determined according to the weighted

histogram analysis method (*15*):

$$P_k = \frac{\sum_j n_{j,k}}{\sum_j N_j f_j c_{j,k}} \qquad f_j = \frac{1}{\sum_k c_{j,k} P_k}$$

where $c_{j,k} = e^{-U_{k,j}/RT}$ and $N_j = \sum_k n_{j,k}$, P_k is the unbiased probability distribution for the kth bin, f_j is the normalization factor for each simulation, $n_{j,k}$ is the counts for the kth bin in the jth simulation, N_j is the total counts stored in the jth simulation, and $U_{j,k}$ is the umbrella potential applied to the kth bin in the jth simulation. A linear combination of continuous basis functions composed of trigonometric and polynomial functions is applied to the discrete version of the potential, i.e., P_k, and a continuous potential of mean force F is obtained from $F_k = -RT \ln P_k$. The adaptive umbrella sampling technique has been implemented in CHARMm and extended to allow for multidimensional sampling of two or more degrees of freedom (*5*).

For this examination of peptide group rotations in vancomycin, standard backbone ϕ and ψ dihedral angles were monitored: ψ_2 involving atoms O−C−C$_\alpha$−C$_\beta$ of residue 2 and ϕ_4 involving atoms H−N−C$_\alpha$−C$_\beta$ of residue 4. These angles were calculated in each saved coordinate set and assigned to one of 36 bins each representing 10° of angle. The umbrella potential was updated 40 times at 50 ps intervals (5 ps of equilibration and 45 ps for the acquisition of statistics) for a total sampling time of 2 ns. The discrete umbrella potential for each torsion angle was made continuous by representation as a linear combination of 24 trigonometric functions plus a constant.

Early results indicated that the carbonyl oxygens of peptide bonds in vancomycin are sterically prohibited from rotating through the macrocycle under normal conditions. Therefore, it is not necessary for us to sample such conformations, and we set an upper limit of 11 kcal/mol for the value of U. This approach is similar to the restriction of range employed in a recent umbrella sampling study of equilibrium properties of protein structures (*16*). The value selected corresponds to an estimated upper bound for peptide group rotation from NMR studies of vancomycin (*4*); 80% of the 1296 bins comprising the final map were below this threshold.

Conformation and Solvent Flux Assessment. To define solvent flux in and out of the binding site, the binding site volume was defined using the following three boundaries: the heavy atoms in the macrocycle rings of vancomycin, the plane defined by atoms C, C$_\alpha$, and N of residue 4 (see Figure 1), and a spherical surface of 8 Å radius centered on atom C$_\alpha$ of residue 4. Water molecules within this boundary were counted in each set of saved coordinates, and a radial distribution function $g(r)$ from C$_\alpha$ of residue 4 was calculated for each bin:

$$g_k(r) = \frac{\bar{N}_k}{V(r)\rho} \quad \text{and} \quad V(r) = \frac{\pi}{3}((r+\Delta r)^3 - r^3)$$

where $V(r)$ is the volume of a quadrant of a sphere (which approximates the binding site volume), $\bar{N}_k$ is the number of waters in the binding site averaged over all coordinates in the kth partition, and ρ is the density of water in units of Å^{-3}. The function was calculated at 1 Å intervals, so that $\Delta r = 1$ Å.

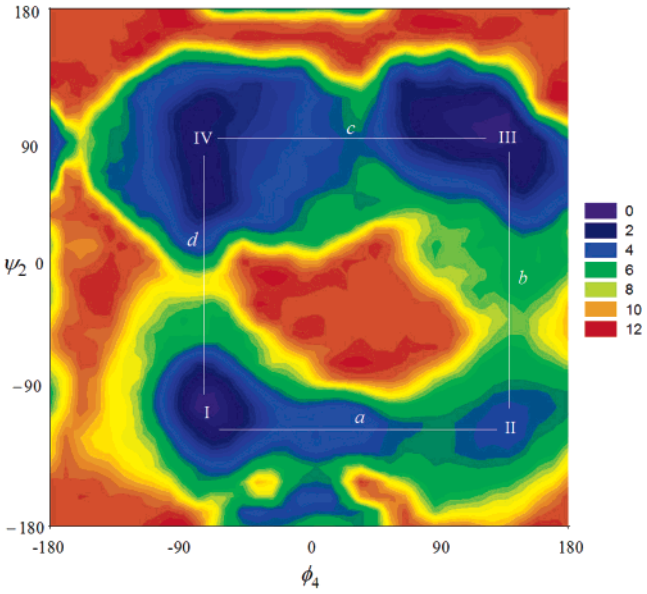

FIGURE 2: Energy contour plot of the peptide plane rotations ψ_2 and ϕ_4. Energy units are in kcal/mol. The four low-energy conformations are marked in roman numerals (I−IV). Pathways linking the four conformers are labeled a−d.

The effect of peptide group rotation on binding site structure was examined by superimposing the coordinate sets in each bin and reorienting them by least-squares fit to the crystal coordinates. The coordinate sets in each bin were averaged to yield a structure of vancomycin corresponding to the ψ_2 and ϕ_4 angle for each bin.

RESULTS

Initial investigations focused on determining the pmf for rotation of ψ_2 because experimental NMR studies have demonstrated that this specific rotation occurs (*4*). It quickly became clear, however, that ϕ_4 rotation was also likely to occur and that a two-dimensional pmf map would be necessary. The map indicates that there are low-energy conformations in four distinct regions (Figure 2). Crystallographic studies invariably show that both of the peptide groups involved are oriented with their hydrogen atoms in the ligand binding site and that they hydrogen bond to the ligand (*14*, *17*−*20*); this structure is located in region II. The other three low-energy conformations result from ~180° rotations of ψ_2 and/or ϕ_4 (Figure 1), and they are about 3−4 kcal/mol lower in free energy than conformation II. Relatively low energy paths exist for individual rotation of ψ_2 and ϕ_4, but simultaneous rotation of both peptide groups is energetically prohibited. Complete 360° rotation of ψ_2 and ϕ_4 is also prohibited; there are relatively low energy paths for the rotation of the amide hydrogens through the macrocycle ring but not for rotation of the carbonyl oxygens through the macrocycle ring. These rotations encountered energetic barriers in excess of 11 kcal/mol and were not, therefore, characterized in detail.

The pmf along the path linking the four low-energy conformations is illustrated in Figure 3. Little in the way of a barrier exists along path a between conformations I and

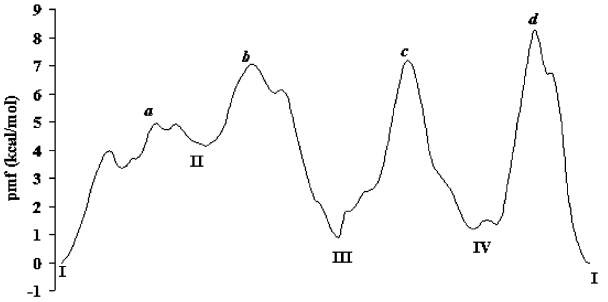

FIGURE 3: The pmf illustrating energetic barriers between the four low-energy conformations (I−IV) along paths a−d of Figure 2.

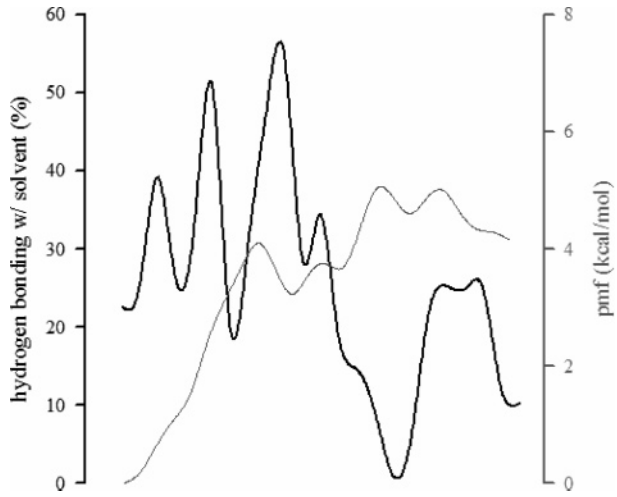

FIGURE 4: Stripping of solvent from the NH group of residue 3 upon passing through the macrocycle. The bold line and left axis represent the percentage of trajectory snapshots in which hydrogen bonding between solvent and the NH group is apparent in bins along path a of Figure 2. The pmf for this path is indicated by the thin line and the right axis. Note that the NH group makes no hydrogen bonds with solvent at the peak of the pmf. At this point, the NH group is in the plane of the macrocycle. Similar results were obtained for the NH group of residue 4.

II, but conformation II has a higher energy than conformation I. The higher energy of conformation II is due to higher mean intramolecular electrostatic energies that arise as a consequence of amide hydrogens from residues 3 and 4 with their partial positive charges positioned in relatively close proximity to each other, to the amide hydrogen of residue 2, and to the quaternary amine of residue 1. Barriers between the other conformations range from 3 to 7 kcal/mol and are more sharply defined.

Interconversion among these conformational states affects the structure of water in an otherwise unoccupied ligand binding site. Since the carbonyl oxygens of residues 2 and 3 are energetically prohibited from passing through the macrocycle, one may infer that water is also unable to pass through the macrocycle. Therefore, any waters that are hydrogen bonded to the amide hydrogens of residues 3 and 4 cannot remain hydrogen bonded, and rotation of the peptide NH group through the macrocycle will be accompanied by desolvation of the amide hydrogens. This process is illustrated in Figure 4 where the prevalence of hydrogen bonds between the amide hydrogen and water is shown for each of the bins along path a in Figure 2. These results indicate that there is no hydrogen bonding between the amide

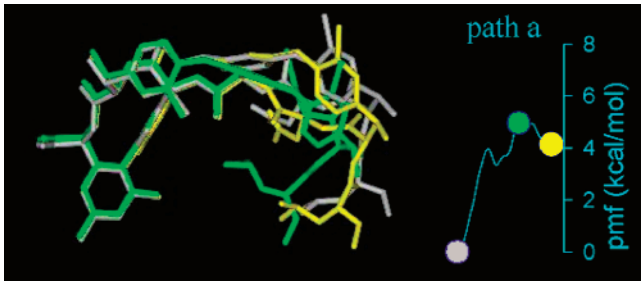

FIGURE 5: Correlation between macrocycle distortion and pmf along path a of Figure 2. Traversing this path entails significant reduction in volume of the ligand binding site.

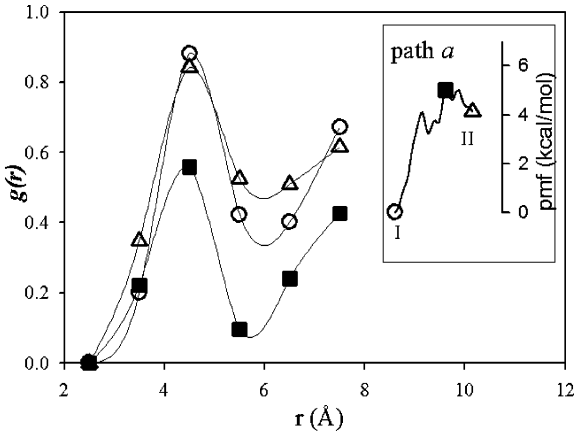

FIGURE 6: Changes in ligand binding site water occupancy along path a of Figure 2, depicted as a radial distribution function for water oxygen atoms centered on atom C_α of residue 4 in vancomycin. Water occupancy decreases as the peptide plane crosses the macrocyclic ring and reaches a minimum at the peak of the pmf. This minimum occurs at the same time that hydrogen bonding with the backbone NH group is precluded. The function amplitude does not reach the values typical of bulk water because vancomycin atoms occupy some of the volume over which the function was integrated.

hydrogen and nearby water molecules when the N−H bond lies in the plane of the macrocyclic ring.

Interconversion among these conformational states also affects the shape of the ligand binding site. Figure 5 illustrates the nature of these shape changes by overlaying average structures from points along path a of Figure 2. When the N−H group of residue 4 rotates into the plane of the macrocyclic ring, the macrocycle rings are distorted and the volume of the binding site is significantly reduced. The reduction of binding site volume is accompanied by an exit of water molecules. As the N−H group rotates out of the plane of the macrocycle ring, the binding site reopens and water molecules situated just outside the binding site re-enter the binding site. The expulsion and re-entry of water is illustrated by radial distribution functions in Figure 6. Along path a from conformation I to II, the radial distribution of water from atom C_α in residue 4 is at a minimum where the pmf is at a maximum, and this corresponds to a loss of approximately 4 of the 10 water molecules from the spherical quadrant over which the radial distribution function was calculated. Figure 4 shows that this point along the pmf corresponds to the point at which no hydrogen bonds form with the amide hydrogen of residue 3. Thus, a point exists along path a at which the pmf is at a maximum, the binding site volume and water molecule content is at a minimum,

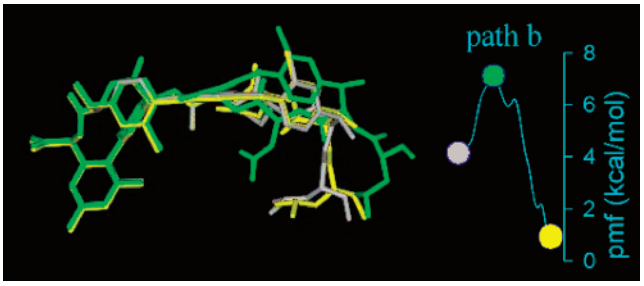

FIGURE 7: Correlation between macrocycle distortion and pmf along path b of Figure 2. Traversing this path entails a significant increase in volume of the ligand binding site.

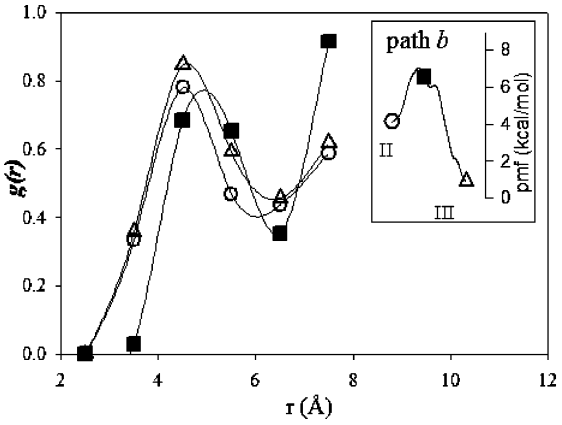

FIGURE 8: Changes in ligand binding site water occupancy along path b of Figure 2. Water occupancy increases as the peptide plane crosses the macrocyclic ring, particularly between 7 and 8 Å from atom C_α of residue 4, and reaches a maximum at the peak of the pmf. This maximum occurs at the same time that hydrogen bonding with the backbone NH group is precluded.

and there are no hydrogen bonds formed with the amide hydrogen of residue 4.

Along path b, there is a larger pmf barrier as the amide hydrogen of residue 3 rotates through the macrocyclic ring (Figure 3). In contrast to path a, however, this barrier is accompanied by an increase in binding site volume (Figure 7). There is a slight decrease and displacement of the first peak in the radial distribution of water molecules (Figure 8), because the side chain of residue 3 (asparagine) enters the binding site and forms a hydrogen bond with the amide hydrogen of residue 3. Waters that might hydrogen bond with this group appear to be displaced by the side chain. It should be recalled that this interaction between the side chain carbonyl group of residue 3 and the amide hydrogens of residues 3 and 4 was also observed in the original crystal structure of vancomycin and was called an "intramolecular surrogate ligand" (*14*). A role for this interaction in desolvating the binding site was suggested at that time, and it appears to be confirmed in these simulations. Beyond 7 Å, there is a clear increase in the amount of water in the binding site.

Spontaneous rotation of the peptide group between residues 3 and 4 does occur in ordinary simulations without umbrella bias. This is the rotation represented by path a, and even though this is not the experimentally observed rotation (*4*), it is reasonable to observe this event in an unbiased simulation before any others because it has the lowest pmf barrier. We also observe that the unbiased simulation persists for a conspicuously long period of time in the region of ϕ_4

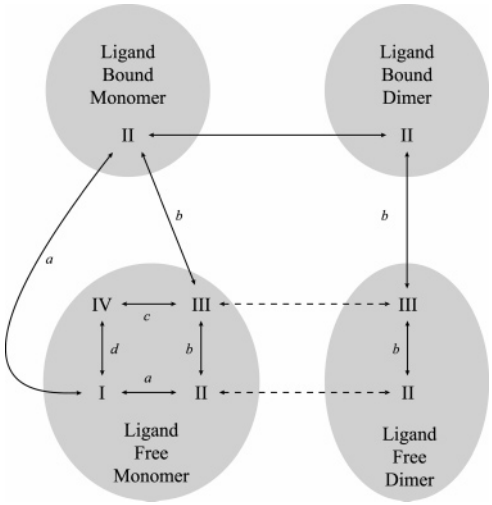

FIGURE 9: Schematic of the interconversions possible between the four low-energy conformations. Monomeric vancomycin may assume any of the four configurations I−IV. Because the peptide group between residues 3 and 4 is involved in dimer formation, dimeric vancomycin may only exist in configurations II and III. Likewise, because both peptide groups between residues 2 and 4 are involved in ligand binding, the ligand bound forms of vancomycin may only exist in configuration II. Path labels a−d correspond to the path labels in Figure 2. The paths between ligand free and ligand bound forms are intended to imply that conversion from conformations I and III to conformation II occurs simultaneously with ligand binding. Solvent stripping helps to preorganize the binding site for ligand, while macrocycle distortions effect solvent and ligand movement into and out of the binding site during these conversions. The paths in dotted lines suggesting dimerization prior to ligand binding are energetically permitted, but they do not preorganize the site for ligand binding. Accordingly, vancomycin should most readily and efficiently bind target moieties if it dimerizes after ligand binding.

$\sim 10°$, which is consistent with the presence of local minima in the middle of path a (Figure 3). The biased and unbiased simulations, therefore, are consistent with each other, and they support the accuracy of adaptive umbrella sampling techniques for determining a pmf.

The pmf results described above indicate that vancomycin monomers will preferentially assume conformations I, III, and IV. Although conformation II is energetically unfavorable, vancomycin must assume conformation II in order to bind ligand. Conversion to conformation II is accompanied by changes in binding site shape and solvation that are remarkable in this context because these changes are prerequisite for ligand binding: they provide for the flux of material into and out of the binding site and for the presentation of desolvated hydrogen bond donors to the ligand. If vancomycin only ever existed in conformation II, these processes would not occur, solvent would most likely exhibit longer residency times bound to hydrogen bond donors in the binding site, and ligand binding would be hindered if not completely precluded.

These considerations lead to a suggestion that ligands enter the vancomycin binding site only when they are in a position to replace water molecules that would otherwise enter when conformations I or III are converting to conformation II (Figure 9). Upon entering the binding site, ligands would be welcomed by one or more hydrogen bond donors freshly desolvated by peptide group rotation. Ligand-free forms in conformation II do not directly bind ligand in this model,

although partial movement along paths a or b followed by a return to conformation II may accomplish as much as full conversion to conformations I or III.

It should be noted that vancomycin forms back-to-back homodimers in which some of the same peptide groups involved in hydrogen bonds to ligands on the "front" side of the molecule also form hydrogen bonds on the "back" side across the dimer interface. Because the peptide group between residues 3 and 4 is involved in hydrogen bonds across the dimer interface, it is not possible for vancomycin *dimers* to adopt conformation I or IV. Presumably, monomers in conformation II or III may dimerize, and ligand may bind to monomers in the dimer as it converts from conformation III to conformation II (Figure 9).

DISCUSSION

Desolvation of a ligand binding site is an absolute prerequisite for molecular recognition. Our results suggest that mechanisms leading to desolvation most likely involve a previously unrecognized level of complexity, preorganization, and synchronization. The simulations provide a detailed perspective on two of these mechanisms, aptly termed "solvent stripping" and "macromolecular breathing". In solvent stripping, water molecules are removed from the amide N−H groups that form hydrogen bonds with ligand by rotating these groups through a macrocycle ring that is too small for water to follow. In macromolecular breathing, water molecules flow in and out of a binding site that is undergoing fluctuations in shape and volume. As the binding site opens and enlarges (Figures 7 and 8), ligands involved in a loose initial binding complex will be drawn into a freshly prepared binding site if they are suitably positioned to replace the solvent water that would be drawn in otherwise.

Our results implicate the backbone peptide group rotations first observed by NMR (*4*) as the slow rate-determining conformational rearrangement observed in stopped-flow studies of vancomycin binding kinetics (*3*). A relationship between these two experimental observations has not been heretofore proposed. We cannot determine whether the molecular events observed in these simulations have an overall positive or negative net effect on ligand binding affinity at this point because they are likely to affect both the forward and reverse binding reactions. Nonetheless, a link between these molecular events and the thermodynamics of cooperativity is likely. Dimerization and ligand binding are thermodynamically cooperative processes in most glycopeptide antibiotics, and a mechanism for this cooperativity has been described that involves the modulation of large-scale vibration modes (*10*, *11*). The present work suggests that dimerization and ligand binding both increase the population of molecules in conformation II, making them structurally congruent processes (*11*) and giving rise to cooperative behavior.

Additional support for this inference is found in the data available for eremomycin, another glycopeptide antibiotic with the same polypeptide backbone structure as vancomycin. Eremomycin has a significantly lower affinity for the target ligand but greater cooperativity between dimerization and ligand binding (*21*). Both of the rotating peptide groups between residues 2 and 4 are involved in hydrogen bonds across the dimer interface in eremomycin, whereas only the peptide group between residues 3 and 4 is involved in the dimer interface of vancomycin. Consequently, dimerization precludes conformations I, III, and IV in eremomycin, but it only precludes conformations I and IV in vancomycin. Thus, the entropic cost of dimerization and ligand binding more completely overlaps in eremomycin than in vancomycin, and this is likely to be manifested as greater cooperativity (*11*). Dimerization itself involves only the convex back surfaces of each monomer. These surfaces may readily desolvate through zippering (*2*) and not require more complex mechanisms.

There is no contradiction between our suggestion that dimer formation inhibits the desolvation process that is prerequisite to ligand binding and the observation that dimer formation and ligand binding are cooperative. There are several kinetic paths by which unliganded monomers may form doubly liganded dimeric complexes, and one may infer from our results that complex formation is most likely to proceed along the paths in which ligand binding precedes dimer formation (Figure 9, solid lines). These paths are entirely plausible on the two-dimensional surface of a bacterial cell, where the likelihood of an encounter between any two monomer−ligand complexes is high relative to the likelihood in solution. This suggestion also implies that there is a logical flaw in the strategy behind recent synthetic efforts aimed at increasing affinity through covalent dimerization (*22*). Covalent linkage of two monomers promotes dimerization because it effectively increases local monomer concentration. Thus, covalent linkage may inhibit desolvation and, hence, ligand binding (*23*). Some covalent dimers do exhibit an improvement in ligand affinity and antimicrobial activity, but the structure−activity relationships are not predictable, suggesting that face-to-face dimerization (*18*) or some other type of ligand-mediated oligomerization mode is responsible for the success that is seen.

The possibility that binding site desolvation in glycopeptide antibiotics proceeds through subtle, multifaceted and synchronized processes prompts us to consider that even more complex mechanisms may operate in large proteins. In acetylcholinesterase, for example, it is difficult to explain how solvent is removed ahead of ligand as it follows the long narrow path from bulk solvent to ligand binding site. Simulations have already suggested a variety of mechanisms in this particular case (*24*), but given the degree of complexity found in vancomycin, the nature of mechanisms operating in large proteins may not yet be fully apparent.

REFERENCES

1. Israelachvili, J. N. (1992) *Intermolecular and Surface Forces*, Academic Press, San Diego.
2. Burgen, A. S. V., Roberts, G. C. K., and Feeney, J. (1975) Binding of Flexible Ligands to Macromolecules, *Nature 253*, 753−755.
3. Popieniek, P. H., and Pratt, R. F. (1991) Kinetics and Mechanism of Binding of Specific Peptides to Vancomycin and Other Glycopeptide Antibiotics, *J. Am. Chem. Soc. 113*, 2264−2270.
4. Waltho, J. P., Williams, D. H., Stone, D. J. M., and Skelton, N. J. (1988) Intramolecular Determinants of Conformation and Mobility within the Antibiotic Vancomycin, *J. Am. Chem. Soc. 110*, 5638−5643.
5. Bartels, C., and Karplus, M. (1997) Multidimensional Adaptive Umbrella Sampling: Applications to Main Chain and Side Chain Peptide Conformations, *J. Comput. Chem. 18*, 1450−1462.
6. Brooks, B. R., Bruccoleri, R. E., Olafson, B. D., States, D. J., Swaminathan, S., and Karplus, M. (1983) CHARMM: A Program

for Macromolecular Energy, Minimization, and Dynamics Calculations, *J. Comput. Chem. 4*, 187−217.
7. Li, D., Sreenivasan, U., Juranic, N., Macura, S., Puga, F. J., II, Frohnert, P. M., and Axelsen, P. H. (1997) Simulated Dipeptide Recognition by Vancomycin, *J. Mol. Recogn. 10*, 73−87.
8. Axelsen, P. H., and Li, D. (1998) A Rational Strategy for Enhancing the Affinity of Vancomycin Towards Depsipeptide Ligands, *Bioorg. Med. Chem. 6*, 877−881.
9. Axelsen, P. H., and Li, D. (1998) Improved Convergence in Dual-Topology Free Energy Calculations Through the Use of Harmonic Restraints, *J. Comput. Chem. 19*, 1278−1283.
10. Jusuf, S., Loll, P. J., and Axelsen, P. H. (2002) The Role of Configurational Entropy in Biochemical Cooperativity, *J. Am. Chem. Soc. 124*, 3490−3491.
11. Jusuf, S., Loll, P. J., and Axelsen, P. H. (2003) Configurational Entropy and Cooperativity between Ligand Binding and Dimerization in Glycopeptide Antibiotics, *J. Am. Chem. Soc. 125*, 3988−3994.
12. Feller, S. E., Zhang, Y., Pastor, R. W., and Brooks, B. R. (1995) Constant Pressure Molecular Dynamics Simulation: the Langevin Piston Method, *J. Chem. Phys. 103*, 4613−4621.
13. Ryckaert, J. P., Ciccotti, G., and Berendsen, H. J. C. (1977) Numerical Integration of the Cartesian Equations of Motion of a System with Constraints: Molecular Dynamics of N-Alkanes, *J. Comput. Phys. 23*, 327−341.
14. Loll, P. J., Bevivino, A. E., Korty, B. D., and Axelsen, P. H. (1997) Simultaneous Recognition of a Carboxylate-Containing Ligand and an Intramolecular Surrogate Ligand in the Crystal Structure of an Asymmetric Vancomycin Dimer, *J. Am. Chem. Soc. 119*, 1516−1522.
15. Kumar, S., Bouzida, D., Swendsen, R. H., Kollman, P. A., and Rosenberg, J. M. (1992) The Weighted Histogram Analysis Method for Free-Energy Calculations on Biomolecules, *J. Comput. Chem. 13*, 1011−1021.
16. Bartels, C., Schaefer, M., and Karplus, M. (1999) Determination of Equilibrium Properties of Biomolecular Systems Using Multidimensional Adaptive Umbrella Sampling, *J. Chem. Phys. 111*, 8048−8067.
17. Schafer, M., Schneider, T. R., and Sheldrick, G. M. (1996) Crystal Structure of Vancomycin, *Structure 4*, 1509−1515.
18. Loll, P. J., Miller, R., Weeks, C. M., and Axelsen, P. H. (1998) A Ligand-Mediated Dimerization Mode for Vanomycin, *Chem. Biol. 5*, 293−298.
19. Loll, P. J., Kaplan, J., Selinsky, B. S., and Axelsen, P. H. (1999) Vancomycin Binding to Low-Affinity Ligands: Delineating a Minimum Set of Interactions Necessary for High-Affinity Binding, *J. Med. Chem. 42*, 4714−4719.
20. Kaplan, J., Korty, B. D., Axelsen, P. H., and Loll, P. J. (2001) The Role of Sugar Residues in Molecular Recognition by Vancomycin, *J. Med. Chem. 44*, 1837−1840.
21. Beauregard, D. A., Maguire, A. J., Williams, D. H., and Reynolds, P. E. (1997) Semiquantitation of Cooperativity in Binding of Vancomycin Group Antibiotics to Vancomycin Susceptible and Resistant Organisms, *Antimicrob. Agents Chemother. 41*, 2418−2423.
22. Nicolaou, K. C., Hughes, R., Cho, S. Y., Winssinger, N., Labischinski, H., and Endermann, R. (2001) Synthesis and Biological Evaluation of Vancomycin Dimers with Potent Activity against Vancomycin-Resistant Bacteria: Target-Accelerated Combinatorial Synthesis, *Chem.—Eur. J. 7*, 3824−3843.
23. Nicolaou, K. C., Cho, S. Y., Hughes, R., Winssinger, N., Smethurst, C., Labischinski, H., and Endermann, R. (2001) Solid- and Solution-Phase Synthesis of Vancomycin and Vancomycin Analogues with Activity against Vancomycin-Resistant Bacteria, *Chem.—Eur. J. 7*, 3798−3823.
24. Axelsen, P. H., Harel, M., Silman, I., and Sussman, J. L. (1994) Structure and Dynamics of the Active Site Gorge of Acetylcholinesterase: Synergistic Use of Molecular Dynamics Simulation and X-ray Crystallography, *Protein Sci. 3*, 188−197.

BI048357T